

Ball-and-Socket Stacking of Supercharged Geodesic Polyarenes: Bonding by Interstitial Lithium Ions

Ivan Arahamian,[†] David Eisenberg,[†] Roy E. Hoffman,[†] Tamar Sternfeld,[†]
Yutaka Matsuo,[‡] Edward A. Jackson,[§] Eiichi Nakamura,[‡] Lawrence T. Scott,[§]
Tuvia Sheradsky,[†] and Mordecai Rabinovitz^{*,†}

Contribution from the Department of Organic Chemistry, The Hebrew University of Jerusalem, Jerusalem 91904, Israel, Department of Chemistry, The University of Tokyo, Hongo, Bunkyo-ku, Tokyo 113-0033, Japan, and Merkert Chemistry Center, Boston College, Chestnut Hill, Massachusetts 02467-3860

Received March 9, 2005; E-mail: mordecai@vms.huji.ac.il

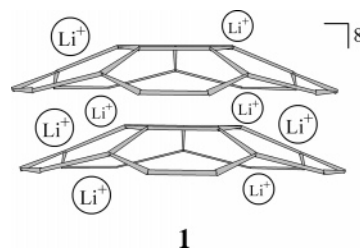
Abstract: Unprecedented supramolecular stacks of highly reduced geodesic π -systems were prepared by the reduction of the derivatized fullerenes $\text{Me}_5\text{C}_{60}\text{H}$ and $\text{Ph}_5\text{C}_{60}\text{H}$ and corannulene with lithium metal ($\text{R}_5\text{C}_{60}^{5-}/\text{Cor}^{4-}/9\text{Li}^+$). The host-guest assemblies form because of the enhanced electrostatic interactions between the lithium cations and the anionic moieties, in addition to the structural compatibility between the curved hydrocarbons. The high stability of these new supramolecular assemblies (heterodimers) enables the introduction of another organization motif to the system. This is achieved by using tethered corannulenes as host molecules, which leads to the formation of tethered bis-heterodimers $((\text{Me}_5\text{C}_{60}^{5-}/\text{Cor}^{4-})_2(\text{CH}_2)_8/18\text{Li}^+)$.

Introduction

The power and beauty of supramolecular chemistry lies in the simplicity with which it provides complex structures that cannot be obtained by traditional synthetic methods. These structures take shape in a manner driven by a broad range of molecular recognition motifs, such as hydrogen bonding, π - π interactions, metal coordination, van der Waals forces, and so forth.¹ Recently there has been increasing interest in organizing fullerenes in supramolecular assemblies, due to their potential applications in chemistry, biology, and material sciences.² In most cases, the supramolecular assemblies are built using host molecules that are capable of recognizing the fullerenes using the complementary principle and concave/convex interactions. The physical properties (e.g., conductivity, magnetism, electronic structure, etc.) of fullerenes can be altered significantly by the addition of electrons to their π -systems.³ Consequently, the properties of supramolecular assemblies formed from fullerene anions will be unique and different from those assembled from neutral ones.

One of the least studied motifs in self-assembly processes is the electrostatic interaction between alkali metal cations and the negatively charged surfaces of reduced polycyclic aromatic hydrocarbons (PAHs).⁴ Such interactions play a dominant role

in the formation of anionic stacked assemblies in the solution phase.⁵ The simplest and best known anionic aggregate in solution is the lithium cyclopentadienide dimer,^{5a} which consists of a supramolecular complex formed by “sandwiching” a lithium cation between two cyclopentadienyl anions. Other instances of aggregation have been reported for more highly charged PAHs, as in the case of the corannulene tetraanion (Cor^{4-}), where an octaanionic dimer is formed ($\text{Cor}^{4-}/\text{Cor}^{4-}/8\text{Li}^+$, **1**),^{5b} and cyclooctabisbiphenylene tetraanion, which forms a highly charged helical tetramer.^{5c}



1

The cases above represent the only fully characterized soluble anionic PAH aggregates found in the literature, and they share two features in common. First, the binding cation is always lithium; second, they are all homodimers (i.e., the anionic

[†] The Hebrew University of Jerusalem.

[‡] The University of Tokyo.

[§] Boston College.

- (1) Lehn, J.-M. *Supramolecular Chemistry: Concepts and Perspectives*; VCH: Weinheim, Germany, 1995.
- (2) (a) Diederich, F.; Gomez-Lopez, M. *Chem. Soc. Rev.* **1999**, 28, 263–277. (b) Guldi, D. M.; Zerbetto, F.; Georgakila, V.; Prato, M. *Acc. Chem. Res.* **2005**, 38, 38–43.
- (3) Reed, C. A.; Bolskar, R. D. *Chem. Rev.* **2000**, 100, 1075–1120.

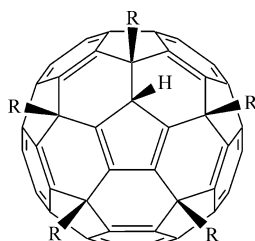
(4) For a recent review about the alkali metal reduction of PAHs, see: Benschafut, R.; Shabtai, E.; Rabinovitz, M.; Scott, L. T. *Eur. J. Org. Chem.* **2000**, 1091–1106 and references therein.

(5) (a) Paquette, L. A.; Bauer, W.; Sivik, M. R.; Bühl, M.; Fiegel, M.; Schleyer, P. v. R. *J. Am. Chem. Soc.* **1990**, 112, 8776–8789. (b) Ayalon, A.; Sygula, A.; Cheng, P.-C.; Rabinovitz, M.; Rabideau, P. W.; Scott, L. T. *Science* **1994**, 265, 1065–1067. (c) Shenhar, R.; Wang, H.; Hoffman, R. E.; Frish, L.; Avram, L.; Willner, I.; Rajca, A.; Rabinovitz, M. *J. Am. Chem. Soc.* **2002**, 124, 4685–4692.

subunits are identical). The scarcity of examples for such self-aggregations in the solution phase makes the study of the phenomenon very difficult. Indeed, the main obstacle thus far has been that the formation of these stacked assemblies is unpredictable and uncontrollable.

An understanding of the underlying principles that would allow a priori predictions of when such supramolecular complexes will form would greatly facilitate the further development and studies on the scope of this phenomenon. If the electrostatic interactions between lithium cations and charged PAHs are ever to be utilized, then they must provide access to a far more diverse array of aggregates, which raises the challenge of creating mixed aggregates (heteroaggregates).

Here we report the reduction of two derivatives of C_{60} , pentamethyl- and pentaphenyl- $C_{60}H$ (**2** and **3**, respectively),⁶ with lithium metal in the presence of corannulene, a process that leads to formation of such supramolecular heterodimers. In these highly charged systems, the anionic partners, Cor^{4-} (host) and the derivatized fullerene pentaanions (guest), are “glued” together by lithium cations in a host–guest assembly ($R_5C_{60}^{5-}/Cor^{4-}/9Li^+$).



2: R = Me

3: R = Ph

The first step in this research was to choose reasonable candidates for aggregation. Two structurally related compounds, a convex fullerene and its smallest curved subunit, corannulene, seemed like good partners, because they are geometrically complementary, and Cor^{4-} was already known to form a supramolecular homodimer.^{5b} Moreover, corannulene is known to function as an efficient electron shuttle in the reduction of fullerenes to their hexaanions.⁷

To promote heteroaggregation of the reduced species, we needed fullerene derivatives in which the charge distribution would not be homogeneous.⁸ The concentration of charge in one segment of the fullerene could enhance the electrostatic interaction with the guest molecule, corannulene, through shared lithium cations and thus increase the likelihood of aggregation. In this regard, fullerene derivatives **2** and **3** held considerable appeal.⁹

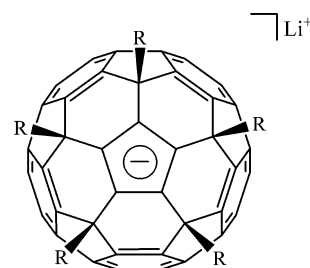
Compounds **2** and **3** are divided into two segments; the first contains a cyclopentadiene (Cp) ring, and the second consists of the remaining 40-carbon π -system, with a central corannulene subunit directly opposite the Cp ring. The Cp undergoes

deprotonation fairly easily yielding a cyclopentadienyl anion,⁶ making it a good candidate as an aggregation site in the solution phase. We were attracted, however, to another possible aggregation site, the corannulene subunit that lies opposite the isolated Cp subunit. A high concentration of charge on this portion of the fullerene might also lead to aggregation.¹⁰

Results and Discussion

Reduction of $Me_5C_{60}H$ and $Ph_5C_{60}H$. Mixtures of corannulene and **2** or **3** were reduced with lithium metal in THF-*d*₈. The diamagnetic species obtained from the reduction were characterized using 1D and 2D NMR methods. When the reduction of **1** or **2** is performed in the absence of corannulene, the process stops at the third reduction stage affording a “trianionic” fullerene,¹¹ whereas the presence of corannulene pushes the reduction further by two steps, yielding a “pentaanionic” fullerene. The reductions of **1** and **2** are very similar, and therefore only the reduction of **1** will be described.

Deprotonation. In the first step of reduction, deprotonation, the color of the solution turns from orange to brown. The deprotonated compound, ($Me_5C_{60}^-/Li^+$, **4a**) (**3** yields **5a**), affords NMR spectra that are similar to those reported in the literature.⁶ It is interesting to note that the ⁷Li NMR spectrum at this stage contains only a single absorption at $\delta = -0.44$ ppm, indicating that the cations are solvent separated ion pairs (SSIPs), in agreement with expectations based on “endohedral homoconjugation”.¹¹ This effect is also responsible for the ease with which the deprotonation occurs using lithium metal, whereas no such reaction takes place with cyclopentadiene itself in THF.



4a: R = Me

5a: R = Ph

Radical States. The deprotonation is followed by three paramagnetic reduction steps ($Me_5C_{60}^{2-}/2Li^+$ (**4b**), $Me_5C_{60}^{3-}/3Li^+$ (**4c**), and $Me_5C_{60}^{4-}/4Li^+$ (**4d**); the color of the solution is green at these stages). The lithium cations are less affected from the paramagnetism of the system, and therefore ⁷Li NMR was used to follow the reduction process. The three paramagnetic

(6) (a) Sawamura, M.; Iikura, H.; Nakamura, E. *J. Am. Chem. Soc.* **1996**, *118*, 12850–12851. (b) Sawamura, M.; Toganoh, M.; Kuninobu, Y.; Nakamura, E. *Chem. Lett.* **2000**, 262–263.

(7) Shabtai, E.; Weitz, A.; Haddon, R. C.; Hoffman, R. E.; Rabinovitz, M.; Khong, A.; Cross, R. J.; Saunders, M.; Cheng, P.-C.; Scott, L. T. *J. Am. Chem. Soc.* **1998**, *120*, 6389–6393.

(8) Although C_{70}^{6-} has the most nonhomogeneous charge distribution in reduced fullerenes, it still does not form a dimer with corannulene. See: Sternfeld, T.; Hoffman, R. E.; Aprahamian, I.; Rabinovitz, M. *Angew. Chem., Int. Ed.* **2001**, *40*, 455–457.

(9) The pentamethyl and -phenyl adducts were chosen for this study, because methyl and phenyl anions are bad leaving groups. The alkali metal reduction of another similar compound, pentafluorenyl $C_{60}H$ led to its dissociation, because fluorenyl anion is a good leaving group; Sternfeld, T. Ph.D. Thesis, The Hebrew University of Jerusalem, Israel, 2003. Similar dissociations were also observed in the CV reduction of other C_{60} monoadducts: Beulen, M. W. J.; Echegoyen, L.; Rivera, J. A.; Herranz, M. A.; Martín-Domenech, A.; Martín, N. *Chem. Commun.* **2000**, 917–918.

(10) DFT calculations conducted on $Me_5C_{60}^-$ (**4**) and $Me_5C_{60}^{5-}$ show that both have two degenerate LUMOs/HOMOs, respectively. This shows that **2** can be reduced to a pentaanion (one of the electrons is in the Cp unit and the others are added to the rest of the π -system). The calculations also show that the atomic orbital coefficients in the LUMOs/HOMOs are the highest around the corannulene subunit, on the opposite side of the derivatization. For semiempirical calculations, see: Chistyakov, A. L.; Stankevich, I. V. *Russ. Chem. Bull.* **1996**, *45*, 2294–2301.

(11) This is in agreement with CV measurements that show only two reduction waves after the deprotonation. See: Iikura, H.; Mori, S.; Sawamura, M.; Nakamura, E. *J. Org. Chem.* **1997**, *62*, 7912–7913.

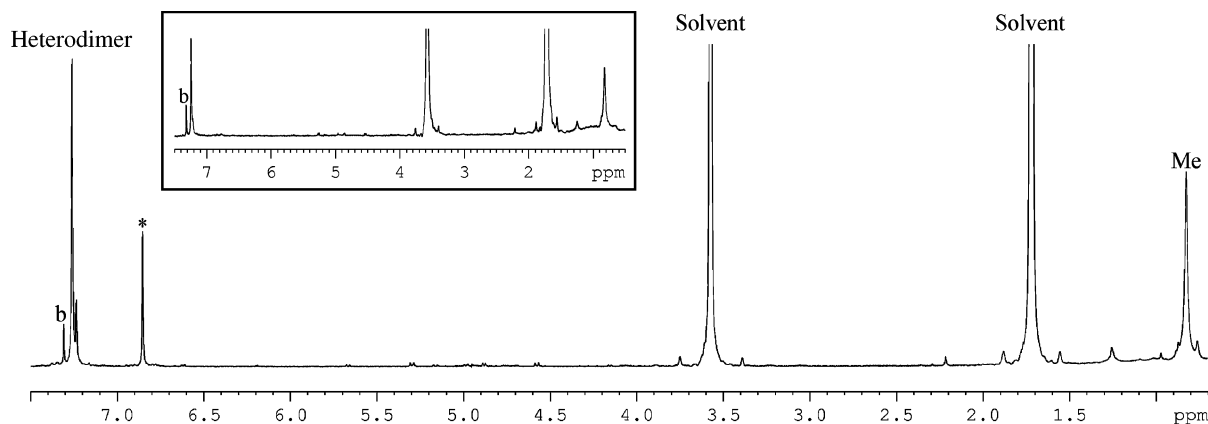
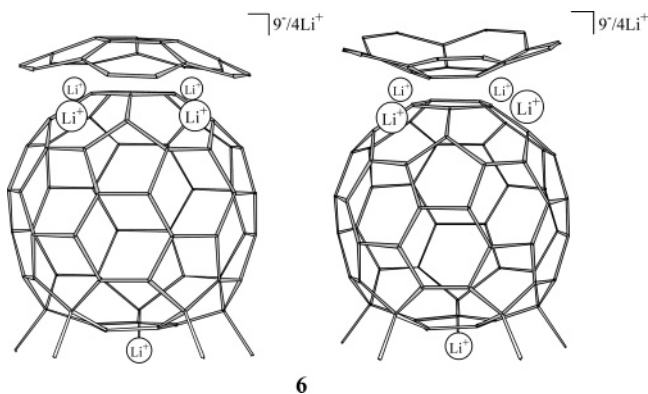


Figure 1. ^1H NMR spectrum of **6** (the reduction was performed in the presence of excess corannulene). In the inset the proton absorptions of **6** can be seen clearly, whereas the corannulene homodimer (*) is yet to be formed ("b" is the absorption of benzene traces).

anions each show a distinct lithium signal in the ^7Li NMR spectra. The high field shifts of these signals show that the "endohedral homoconjugation" found in **4a** has diminished and even disappeared (the Cp anion does not disperse its charge). The third stage of reduction, **4c**, shows also a relatively broad peak in the ^1H NMR spectrum ($\delta = 0.51$ ppm), which corresponds to the protons of the methyl groups (no ^1H NMR was observed for **4b** or **4d**). The occurrence of this signal presumably results from a singlet–triplet equilibrium in **4c**.

Dimerization. The fifth stage of reduction is the most important and fascinating. At this stage, a supramolecular aggregate between Cor^{4-} and fullerene pentaanion is formed ($\text{Me}_5\text{C}_{60}^{5-}/\text{Cor}^{4-}/9\text{Li}^+$, **6**; the color of the solution changes from green to black). The formation of this assembly is revealed by the following NMR data.



The ^1H NMR spectrum of **6** consists of three peaks (Figure 1). Two of the peaks appear at low field, $\delta = 7.27$ and 7.24 ppm, with relative intensities of approximately 3:1. The third peak, which is relatively broad, appears at high field, $\delta = 0.82$ ppm. When corannulene is used in excess (relative to **2** or **3**),¹² the peak from its tetraanionic homodimer, $\delta = 6.85$ ppm,^{5b} shows up only after the two peaks at low field reach their maximum height (Figure 1). This means that the two peaks at low field belong to corannulene entities that do not form supramolecular dimers with other corannulenes. Thus, these new corannulene entities appear to be favored over the corannulene homodimer, because their formation preempts the homodimerization of corannulene.

The ^7Li NMR spectra of **6** offer compelling independent evidence for an aggregation process at this stage (Figure S1, Supporting Information). The spectrum at 165 K consists of three main peaks that appear around $\delta = -0.18$, -7.36 , and -12.86 ppm.¹³ The highly shifted lithium absorptions ($\delta = -12.86$ ppm) are diagnostic for lithium cations sandwiched between aromatic anionic layers.⁵

When the temperature is increased, all the lithium peaks coalesce and give rise to a broad peak at $\delta = -5.91$ ppm, except for the peak at $\delta = -7.36$ that remains unaffected. This dynamic process corresponds to the exchange between lithium cations trapped between the anionic layers (highly shifted ones) and those on the outside (relatively low field). The exchange barriers of the dynamic processes were measured using NMR exchange spectroscopy (EXSY)¹⁴ and found to be between 8.337 ± 0.022 and 10.474 ± 0.304 kcal/mol. The constant peak at $\delta = -7.36$ ppm has been assigned to the cation of Cp based on the chemical shifts measured previously for the same anion, in the stages before the dimerization.

The ^{13}C NMR spectrum of **6** (Figure 2) shows three sets of multiplied absorptions, with chemical shifts that are very close to those from the carbons of the corannulene homodimer (Figure 2A).^{5b} These multiplied absorptions belong to new tetraanionic corannulene entities. The spectrum also contains some of the carbon peaks of the fullerene itself. The full carbon spectrum of the fullerene subunit of **6** (Figure 2B) was measured using a ^{13}C -enriched sample. These carbon absorptions were assigned using 2D NMR incredible natural abundance double quantum transfer experiment (INADEQUATE) (this was performed only for ^{13}C -enriched **2** and the anions derived from it).¹⁵ The carbon chemical shifts of the fullerene moiety are shifted slightly to high field relative to the carbons of the deprotonation product, **4**. It is important to note that carbon C3 (Figure 3), which was shifted to low field ($\delta = 162.3$ ppm) in **4** due to "endohedral homoconjugation", is shifted now to higher field ($\delta = 148.2$ ppm) with the rest of the fullerene carbons, again confirming that the homoconjugation is lessened by reduction. Moreover, carbons C7 and C8 ($\delta = 131.6$ and 115.9 ppm) that reside on the corannulene subunit of the fullerene on the opposite side of

(12) The solution contained 6.0×10^{-3} M of corannulene and 3.7×10^{-3} M of **2** or 2.7×10^{-3} M of **3**.

(13) These values are taken from a sample of **6** that does not contain any excess corannulene (no corannulene homodimer is present). This means that these chemical shifts belong only to the lithium cations of **6**.

(14) Perrin, C. L.; Dwyer, T. J. *Chem. Rev.* **1990**, *90*, 935–967.

(15) Bax, A.; Freeman, R. *J. Magn. Reson.* **1980**, *41*, 507–511.

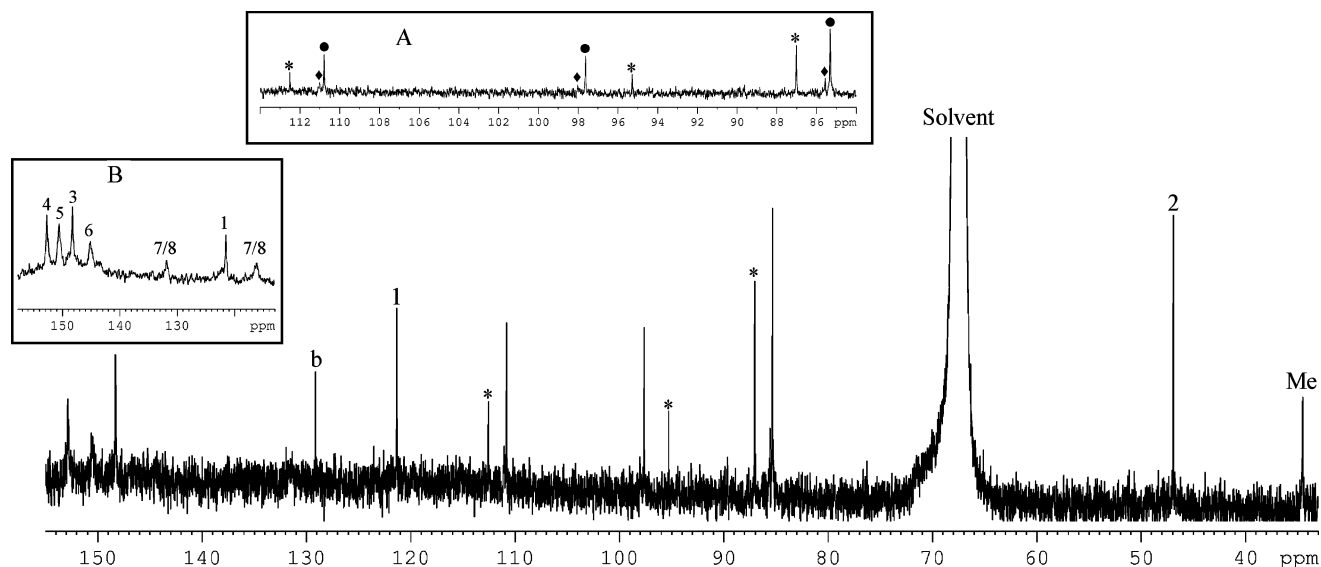


Figure 2. ^{13}C NMR of **6** (the reduction was performed in the presence of excess corannulene). Inset “A” is an expansion on the carbon absorptions of the different corannulene entities; homodimer (*), major heterodimer (●), and minor heterodimer (◆). Inset “B” shows the carbon absorptions of the fullerene subunit of **6** (^{13}C -enriched sample) (“b” is the absorption of benzene traces).

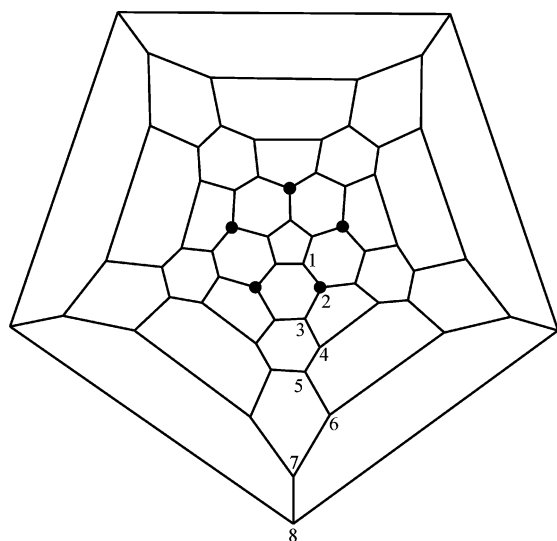


Figure 3. Schlegel diagram of anions **4a–d**, **5a–d**, **6**, **7**, and **9**. The substituents (●) are connected to carbon atoms type 2.

the Cp anion ($\delta = 121.3$ ppm) are the most shifted to high field, due to concentration of charge on them.

Further evidence for the formation of the heterodimers comes from self-diffusion experiments.¹⁶ These experiments show that the methyl protons of the derivatized fullerene and the peak of the corannulene proton diffuse at the same rate in solution ($D_{257\text{ K}} = 1.8 \pm 0.1 \times 10^{-10}$ m²/s for both isomers).¹⁷ Such behavior is expected only if the two systems constitute parts of a single entity.

Temperature-dependent ^1H NMR measurements showed that the two peaks belonging to the two new corannulene entities ($\delta = 7.27$ and 7.24 ppm) undergo coalescence at high temperatures. This means that there is a dynamic process that exchanges the environments of these two protons. The $\Delta G_{278\text{ K}}^\ddagger$ of the process is 15.0 ± 0.2 kcal/mol and 14.0 ± 0.2 kcal/mol

for the inverse process.¹⁸ Most likely, the dynamic process stems from the bowl-to-bowl inversion of the corannulene subunit.¹⁹ Such an inversion process can yield two diastereomers of the heterodimer (e.g., *concave–convex* and *convex–convex* interactions).²⁰

The question remains as to the full structure of the dimers: where is the corannulene located on the derivatized surface of the fullerene? The high symmetry of the dimers, as observed by NMR, demands that the C_5 rotational axes of the two partners must coincide, at least on a time-averaged basis, if not permanently. This leaves only two possibilities. The corannulene could be associated either at the derivatized end of the fullerene, over the isolated Cp anion moiety, or at the opposite end, over a corannulene subunit. According to the ^1H and ^7Li NMR spectra, the complexation site is not the Cp anion but rather the corannulene subunit on the opposite side (**6**).

First, although two isomers are formed, only a single methyl peak can be seen in the ^1H NMR spectrum, even at low temperatures. This means that the methyl groups are located far enough from the corannulene unit not to be significantly affected by the dynamic process and so show only a single broad absorption.

To probe this issue further, two substituted corannulenes, *tert*-butyl- and methylcorannulene, were separately reduced with **2**. Both corannulene derivatives afforded the same types of heterodimers as corannulene, but in neither of them did the fullerene methyl peak split or lose symmetry. Moreover, the chemical shifts of the methyl groups hardly changed in these aggregates, and no NOE interactions were found between the two layers. This shows that the methyl groups are far enough removed from the complexation site that they are not perceptibly affected by the dynamic process and cannot experience any NOE from the corannulene substituents.

(18) Kost, D.; Carlson, E. H.; Raban, M. *J. Chem. Soc., Chem. Commun.* **1971**, 656–657.

(19) (a) Scott, L. T.; Hashemi, M. M.; Bratcher, M. S. *J. Am. Chem. Soc.* **1992**, *114*, 1920–1921. (b) Borchardt, A.; Fuchicello, A.; Kilway, K. V.; Baldrige, K. K.; Siegel, J. S. *J. Am. Chem. Soc.* **1992**, *114*, 1921–1923.

(20) Wang, Z.; Dötz, F.; Enkelmann, V.; Müllen, K. *Angew. Chem., Int. Ed.* **2005**, *44*, 1247–1250.

(16) Cohen, Y.; Avram, L.; Frish, L. *Angew. Chem., Int. Ed.* **2005**, *44*, 520–554 and references therein.

(17) The diffusion constant of the homodimer of corannulene tetraanion in the same conditions is $D_{257\text{ K}} = 2.2 \pm 0.1 \times 10^{-10}$ m²/s.

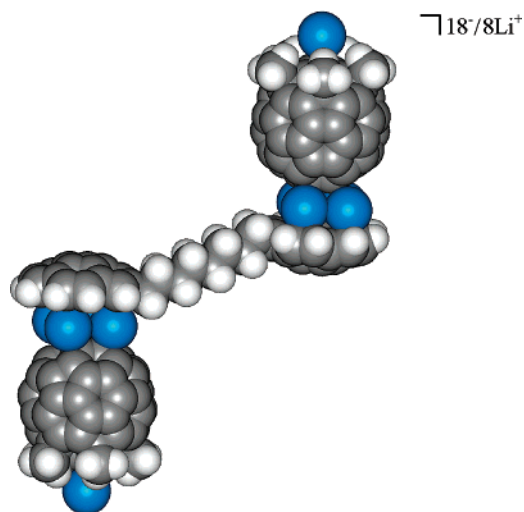


Figure 4. Space-filling model of one of the possible structures of the bis-heterodimer, **9**. The blue spheres represent contact lithium cations.

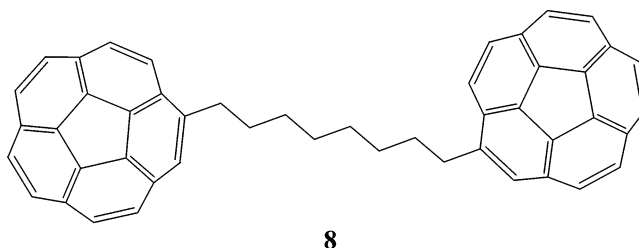
Comparisons between the ^1H NMR spectra of the heterodimers **6** and **7** ($\text{Ph}_5\text{C}_{60}^{5-}/\text{Cor}^{4-}/9\text{Li}^+$) further support this conclusion. In **7**, the proton chemical shifts of the complexed corannulenes ($\delta = 7.31$ and 7.28 ppm) closely match those in **6** ($\delta = 7.27$ and 7.24 ppm). Changing the five-fullerene substituents from methyls to phenyls would be expected to have a much greater effect on the chemical shifts of the corannulene hydrogens if complexation were occurring at the derivatized pole of the fullerene.

In the ^7Li NMR spectra, the lithium absorption of the cation attached to the Cp anion of **6** ($\delta = -7.3$ ppm) is not dependent on temperature.²¹ Moreover, no exchange was measured for this lithium absorption in the EXSY experiments. This means that the Cp ring is positioned far from the complexation site, because the cation attached to it does not participate in the dynamic process found in the heterodimer.

Bis-Heterodimer. The higher stability of the heterodimers **6** and **7**, relative to the homodimer **1**, enables the introduction of another organization motif in the formation of these complexes. It is possible to use the corannulenes as templates to construct heterodimers that are arranged in a specific shape. Tethering corannulene units together in different shapes can accomplish this.

To show that this concept works, a mixture of **2** and 1,8-dicorannulenyl octane (**8**) was reduced with lithium metal. It has been previously shown that the reduction of **8** with lithium metal affords an intramolecular (and not an intermolecular) homodimer, and no mixed dimer between **8** and corannulene could be formed.²² In this case, however, the formation of the heterodimer is favorable, and thus the reduction of **2** and **8** affords only a chiral supramolecular assembly consisting of two heterodimers linked together by an octamethylene chain ($(\text{Me}_5\text{C}_{60}^{5-}/\text{Cor}^{4-})_2(\text{CH}_2)_8/18\text{Li}^+$), **9**, Figure 4). This bis-heterodimer has a charge of 18 electrons all together, making it the highest charged PAH system ever to be observed in solution. The fact that tethering does not affect the ability of the

corannulene to form these heterodimers means that tethered corannulenes can indeed function as templates on which the heterodimers can form.



Conclusions and Outlook

In this study, we demonstrated that the electrostatic interactions found between charged PAHs and lithium cations can be put to use for the construction of supramolecular complexes. It was also shown that it is possible to predict a priori when such supramolecular aggregates will form. In addition, it is now evident that diverse aggregates can be formed if structural compatibility between the different components is arranged. The fact that the dimerization takes place on the corannulene subunit side means that the Cp anion on the opposite side remains free. Consequently, it is available for the formation of functional supramolecular assemblies, such as transition metal complexes,²³ that can be used as catalytic agents. Moreover, it should be possible to exchange the methyl or phenyl side groups for other appropriate groups that could lead to the formation of anionic liquid crystals.²⁴ Tethering to make hosts and guests that are both “divalent” (cf. **8**) will open the door to the formation of highly charged supramolecular oligomers and polymers. All of these possibilities and more ensure the further development of these fascinating heterodimers and their potential applications in diverse disciplines.

Experimental Section

The 1D and 2D NMR spectra were recorded on a Bruker DRX-400 pulsed FT spectrometer operating at 400.13, 100.62, and 155.51 MHz for ^1H , ^{13}C , and ^7Li NMR, respectively. The ^1H and ^{13}C NMR chemical shifts were measured relative to the most downfield THF- d_8 peak (3.57 and 67.39 ppm, respectively, relative to TMS). The ^7Li spectrum was referenced to the frequency of the ^1H signal of dilute TMS in THF- d_8 (inferred from the ^1H solvent frequency) multiplied by IUPAC's $\Xi/100$ value of 0.38863797.²⁵ The temperature was calibrated with methanol.²⁶ The DFT calculations were conducted using B3LYP/6-31G* level of theory.^{27,28}

Diffusion NMR. The diffusion coefficients were measured using the pulsed field gradient stimulated spin-echo (PGSTE) technique.¹⁶ The measurements were carried out in a sealed extended 4-mm-diameter

(21) One peak is observed because the Cp anion is far removed from the complexation site, and therefore the dynamic process does not affect the peak significantly.

(22) Shabtai, E.; Hoffman, R. E.; Cheng, P.-C.; Bayrd, E.; Preda, D. V.; Lawrence, L. T.; Rabinovitz, M. *J. Chem. Soc., Perkin Trans. 2* **2000**, 129–133.

- (23) (a) Sawamura, M.; Kuninobu, Y.; Nakamura, E. *J. Am. Chem. Soc.* **2000**, *122*, 12407–12408. (b) Sawamura, M.; Kuninobu, Y.; Toganoh, M.; Matsuo, Y.; Yamanaka, M.; Nakamura, E. *J. Am. Chem. Soc.* **2002**, *124*, 9354–9355. (c) Kuninobu, Y.; Matsuo, Y.; Toganoh, M.; Sawamura, M.; Nakamura, E. *Organometallics* **2004**, *23*, 3259–3266.
- (24) Sawamura, M.; Kawai, K.; Matsuo, Y.; Kanie, K.; Kato, T.; Nakamura, E. *Nature* **2002**, *419*, 702–705.
- (25) Harris, R. K.; Becker, E. D.; Cabral de Menezes, S. M.; Goodfellow, R.; Granger, P. *Magn. Reson. Chem.* **2002**, *40*, 489–505.
- (26) Ammann, C.; Meier, P.; Merbach, A. E. *J. Magn. Reson.* **1982**, *46*, 319–321.
- (27) Frisch, M. J. et al. *Gaussian 98*, revision A.9; Gaussian, Inc.: Pittsburgh, PA, 1998.
- (28) (a) Krishnan, R.; Binkley, J. S.; Seeger, R.; Pople, J. A. *J. Chem. Phys.* **1980**, *72*, 650–654. (b) Becke, A. D. *J. Chem. Phys.* **1993**, *98*, 5648–5652.

Pyrex tube inserted into a regular 5-mm-diameter NMR glass tube (to reduce convection due to sample heating by the RF pulses) at 257.5 ± 0.5 K.

Preparation of the Reduction Samples. All the samples, except those for the diffusion measurements, were reduced in 5-mm-diameter NMR glass tubes equipped with an upper reduction chamber. The fullerene derivatives, **2** or **3** (3 mg), were introduced into the lower chamber of the tube under an argon atmosphere. Afterward, an appropriate amount of corannulene or its derivatives (0–1.5 mg) was added to the lower chamber. Lithium metal (kept in paraffin oil, cleansed from the oxidized layer, and rinsed in petroleum ether 40–60 °C) was introduced under argon to the reduction chamber as a wire. The tube was then placed under high vacuum and dried by flame. Approximately 1 mL of anhydrous THF-*d*₈ (dried over a sodium/potassium alloy under high vacuum) was vacuum-transferred to the NMR tube and was degassed several times. Finally, the tube was flame-sealed under high vacuum.

Controlled Reduction Process. The reduction took place when the THF-*d*₈ solution was brought into contact with the metal by inverting the sample in solid dry ice. Reduction was stopped by returning the sample to the upright position, separating the metal from the solution. The formation of the anions was detected visually by the change in the color of the solution and by ¹H and ⁷Li NMR spectroscopies.

NMR Data. Me₅C₆₀[−]/Li⁺ (**4a**): ¹H NMR (THF-*d*₈, 260 K) δ 2.39 (s); ¹³C NMR (THF-*d*₈, 260 K) δ 162.28 (C3), 148.96 (C8), 148.89 (C4), 146.98 (C6), 146.01 (C7), 142.98 (C5), 130.25 (C1), 54.61 (C2), 31.68 (C-methyl); ⁷Li NMR (THF-*d*₈, 220 K) δ −0.44.

Me₅C₆₀^{2−}/2Li⁺ (**4b**): ⁷Li NMR (THF-*d*₈, 200 K) δ −6.18 (Cp).

Me₅C₆₀^{3−}/3Li⁺ (**4c**): ¹H NMR (THF-*d*₈, 260 K) δ 0.51 (s); ⁷Li NMR (THF-*d*₈, 165 K) δ −8.34 (Cp).

Me₅C₆₀^{4−}/4Li⁺ (**4d**): ⁷Li NMR (THF-*d*₈, 200 K) δ −6.82 (Cp).

Me₅C₆₀^{5−}/Cor^{4−}/9Li⁺ (**6**): ¹H NMR (THF-*d*₈, 240 K) δ 7.27 (s, 10H, isomer1), 7.24 (s, 3H, isomer2), 0.82 (s, 17H, methyl); ¹³C NMR (THF-*d*₈, 260 K) δ 152.72 (C4), 150.47 (C5), 147.28 (C3), 145.08 (C6), 131.65 (C7/C8), 121.39 (C1), 115.90 (C8/C7), 111.02 (C-cor-isomer2), 110.77 (C-cor-isomer1), 98.02 (C-cor-isomer2), 97.62 (C-cor-isomer1), 85.56 (C-cor-isomer2), 85.31 (C-cor-isomer1), 46.81 (C2), 34.49 (C-methyl); ⁷Li NMR (THF-*d*₈, 165 K) δ −0.18, −4.25, −6.17, −7.36, −12.86, −14.00, −15.40.

The carbon chemical shifts of C7 and C8 could not be fully assigned, due to the broadness of the peaks.

Ph₅C₆₀[−]/Li⁺ (**5a**): ¹H NMR (THF-*d*₈, 220 K) δ 7.85 (m, 10H, *ortho*), 7.06 (m, 15H, *meta* and *para*); ¹³C NMR (THF-*d*₈, 220 K) δ 159.92 (C3), 149.36 (C8), 149.23 (C4), 147.19 (C6), 146.44 (C7), 145.93 (C-phenyl), 143.10 (C5), 129.09 (C-*ortho*), 128.71 (C1), 128.25 (C-*meta*), 126.38 (C-*para*), 62.15 (C2), 31.7; ⁷Li NMR (THF-*d*₈, 220 K) δ −0.14.

The carbon chemical shifts of **4a** were used to assign most of the carbons of the fullerene subunit of **5a**. The rest were assigned using 2D NMR methods.

Ph₅C₆₀^{3−}/3Li⁺ (**5c**): ¹H NMR (THF-*d*₈, 240 K) δ 6.84–6.47 (m, phenyl peaks); ⁷Li NMR (THF-*d*₈, 165 K) δ −6.34.

Ph₅C₆₀^{5−}/Cor^{4−}/9Li⁺ (**7**): ¹H NMR (THF-*d*₈, 240 K) δ 7.31 (s, 10H, isomer1), 7.28 (s, 5H, isomer2), 6.98 (d, 15H, *ortho1*), 6.86 (d, 5H, *ortho2*), 6.52 (m, 10H, *para* and *para2*), 6.45 (m, 15H, *meta* and *meta2*); ¹³C NMR (THF-*d*₈, 240 K) δ 154.19 (C60), 152.89 (C-phenyl1), 149.76 (C60), 148.68 (C60), 147.93 (C-phenyl2), 128.81 (C-*ortho2*), 128.68 (C-*ortho1*), 126.29 (C-*meta2*), 125.95 (C-*meta1*), 123.84 (C-*para2*), 123.08 (C-*para1*), 111.14 (C-cor-isomer2), 110.80 (C-cor-isomer1), 98.25 (C-cor-isomer2), 97.69 (C-cor-isomer1), 85.85 (C-cor-isomer2), 85.52 (C-cor-isomer1), 55.59 (C2-isomer1), 53.69 (C2-isomer2); ⁷Li NMR (THF-*d*₈, 165 K) δ −0.12, −6.01, −7.22, −12.98, −15.25.

The Δ*G*_{285 K}[‡] of the dynamic process observed in the ¹H NMR is 15.0 ± 0.2 and 14.5 ± 0.2 kcal/mol for the inverse process.

(Me₅C₆₀^{5−}/Cor^{4−})₂(CH₂)₈/18Li⁺ (**9**): ¹H NMR (THF-*d*₈, 265 K) δ 7.32–7.02 (corannulene moiety), 5.28 (bridge peak), 4.19 (bridge peak),

2.62–2.46 (bridge peaks), 0.83 (s, methyl); ¹³C NMR (THF-*d*₈, 265 K) δ 152.48 (C4), 150.35 (C5), 148.11 (C3), 144.77 (C6), 132.08 (C7/C8), 121.42 (C1), 116.19 (C8/C7), 85.62–83.70 (corannulene moiety), 46.93 (C2), 34.4 (C-methyl); ⁷Li NMR (THF-*d*₈, 180 K) δ −0.74, −7.20, −12.87, −15.39.

Assignment of the carbon chemical shifts carbons of the fullerene subunit of **9** is based on the assignment in **6**.

Methylcorannulene. Into an oven-dried 25-mL round-bottom flask containing a stirring bar were added 120 mg (0.365 mmol) of bromocorannulene and 39.5 mg (0.0729 mmol) of [1,3-bis(diphenylphosphino)propane]dichloronickel [NiCl₂(dppp)]. The flask was then fitted with an oven-dried condenser and purged with nitrogen. To this solid mixture was added 15 mL of anhydrous tetrahydrofuran, and 0.61 mL of a 3.0 M solution (1.8 mmol) of methylmagnesium bromide in tetrahydrofuran was then added dropwise by syringe. An additional 2 mL of dry tetrahydrofuran were used to rinse the condenser. The flask was then lowered into a preheated silicon oil bath at 75 °C, and the solution was kept at reflux overnight. The reaction mixture was quenched with 50 mL of 10% HCl solution and extracted with methylene chloride three times. The combined extracts were then washed once with 10% HCl solution and once with brine. The methylene chloride layer was dried with magnesium sulfate and filtered. Removal of the solvent under reduced pressure gave an off-white solid, which was purified on a column of silica gel with a 1:19 methylene chloride/hexane solvent system to give 60.9 mg (63% yield) of methylcorannulene as a white solid. ¹H NMR (CDCl₃) δ 7.92 (d, *J* = 8.8 Hz, 1H), 7.84 (d, *J* = 8.8 Hz, 1H), 7.81 (s, 2H), 7.78 (s, 2H), 7.78 (d, *J* = 8.8 Hz 1H), 7.73 (d, *J* = 8.8 Hz, 1H), 7.57 (s, 1H), 2.83 (s, 3H). MS *m/z* (rel intensity): 264 (100, M⁺), 263 (99, M⁺ − H), 248 (2), 131 (12).

Me₅C₆₀^{5−}/MeCor^{4−}/9Li⁺. ¹H NMR (THF-*d*₈, 220 K) δ 7.34 (d, 1H, cor), 7.24 (d, 2H, cor), 7.18 (m, 3H, cor), 7.11 (d, 1H, cor), 7.08 (d, 1H, cor), 7.03 (s, 1H, cor), 3.57 (s, cor-methyl, isomer1), 3.52 (s, cor-methyl, isomer2), 0.83 (s, methyl); ¹³C NMR (THF-*d*₈, 240 K) δ 148.48 (C3), 121.55 (C1), 89.41–83.44 (C-cor), 47.18 (C2), 34.22 (C-methyl), 21.96 (C-corannulene methyl, both isomers); ⁷Li NMR (THF-*d*₈, 165 K) δ −0.31, −6.19, −7.38, −12.86, −15.32.

The ¹³C NMR absorptions are from the 2D NMR experiments (HSQCSI and HMBC).

tert-Butylcorannulene. In a 5-mL pear-shaped flask equipped with a magnetic stirrer and a rubber septum were placed 20 mg (0.08 mmol) of corannulene and 1.0 mL of freshly distilled ether. To this solution, 0.047 mL of a 1.7 M solution of *tert*-butyllithium in pentane (0.08 mmol) was added dropwise. The resulting purple suspension was stirred for 6 h at room temperature and then quenched with 5 mL of water and extracted with 3 × 10 mL of CH₂Cl₂. The crude product was then treated with 29.5 mg (13 mmol) of 2,3-dichloro-5,6-dicyano-1,4-benzoquinone (DDQ) in 4.0 mL of refluxing benzene for 5 h. Cooling the reaction mixture and removing the solvent under reduced pressure gave crude material that was chromatographed on silica gel using hexane ethyl acetate (10:1) as eluant. The products were further purified via silica gel preparative TLC with pentane/methylene chloride (3:1) to afford 4.5 mg (18% yield) of *tert*-butylcorannulene as a sticky yellow solid: ¹H NMR (CDCl₃) δ 8.26 (d, *J* = 9.0 Hz, 1H), 7.79 (m, 8H), 1.71 (s, 9H). MS *m/z* (rel intensity): 306 (46, M⁺), 291 (100), 276 (45), 261 (6), 250 (14), 224 (3), 132 (14). HRMS Calcd. for C₂₄H₁₈ (M⁺): 306.1408. Found: 306.1412.

Me₅C₆₀^{5−}/*tert*-BuCor^{4−}/9Li⁺. ¹H NMR (THF-*d*₈, 240 K) δ 7.51 (d, 1H, cor), 7.46 (d, 1H, cor), 7.33 (s, 1H, cor), 7.35 (d, 1H, corannulene peak), 7.29 (d, 1H, cor), 7.20–7.15 (m, 4H, cor), 2.16 (s, 9H, *tert*-butyl, isomer1), 2.14 (s, *tert*-butyl, isomer2), 0.83 (s, methyl); ¹³C NMR (THF-*d*₈, 240 K) δ 148.28 (C3), 121.60 (C1), 89.54–84.62 (C-cor), 47.17 (C2), 33.99 (C-methyl), 33.3 (C-*tert*-butyl, both isomers); ⁷Li NMR (THF-*d*₈, 180 K) δ −0.45, −6.13, −7.34, −12.84, −15.53.

The ¹³C NMR absorptions are from the 2D NMR experiments (HSQCSI and HMBC).

Acknowledgment. We thank Silvio Biali, Yoram Cohen, and Jay S. Siegel for fruitful discussions. We thank Peichao Cheng for a sample of *tert*-butylcorannulene and Eric Bayrd for a sample of 1,8-dicorannuleneyoctane. This work was supported by the United States–Israel Binational Science Foundation (BSF), the Israeli Science Foundation (Grant No. 147/00), and the U.S. Department of Energy. I.A. is thankful for the Horowitz Foundation Scholarship.

Supporting Information Available: Details of the EXSY experiment (results summarized in Supporting Table 1) and discussion about the dynamic process. The ^7Li NMR spectrum of **6** (Supporting Figure 1). Complete citation for ref 27 and additional references. This material is available free of charge via the Internet at <http://pubs.acs.org>.

JA0515102